

Understanding the Charge Carrier Conduction Mechanisms of Plasma-Polymerized 2-Furaldehyde Thin Films via DC Electrical Studies

Kabir, Humayun; Bhuiyan, A.h.; Rahman, M. Mahbubur

DOI:

[10.1016/j.tsf.2016.04.033](https://doi.org/10.1016/j.tsf.2016.04.033)

License:

Creative Commons: Attribution-NonCommercial-NoDerivs (CC BY-NC-ND)

Document Version

Peer reviewed version

Citation for published version (Harvard):

Kabir, H, Bhuiyan, AH & Rahman, MM 2016, 'Understanding the Charge Carrier Conduction Mechanisms of Plasma-Polymerized 2-Furaldehyde Thin Films via DC Electrical Studies', *Thin Solid Films*.

<https://doi.org/10.1016/j.tsf.2016.04.033>

[Link to publication on Research at Birmingham portal](#)

Publisher Rights Statement:

Checked May 2016

General rights

Unless a licence is specified above, all rights (including copyright and moral rights) in this document are retained by the authors and/or the copyright holders. The express permission of the copyright holder must be obtained for any use of this material other than for purposes permitted by law.

- Users may freely distribute the URL that is used to identify this publication.
- Users may download and/or print one copy of the publication from the University of Birmingham research portal for the purpose of private study or non-commercial research.
- User may use extracts from the document in line with the concept of 'fair dealing' under the Copyright, Designs and Patents Act 1988 (?)
- Users may not further distribute the material nor use it for the purposes of commercial gain.

Where a licence is displayed above, please note the terms and conditions of the licence govern your use of this document.

When citing, please reference the published version.

Take down policy

While the University of Birmingham exercises care and attention in making items available there are rare occasions when an item has been uploaded in error or has been deemed to be commercially or otherwise sensitive.

If you believe that this is the case for this document, please contact UBIRA@lists.bham.ac.uk providing details and we will remove access to the work immediately and investigate.

Accepted Manuscript

Understanding the Charge Carrier Conduction Mechanisms of Plasma-Polymerized 2-Furaldehyde Thin Films via DC Electrical Studies

Humayun Kabir, A.H. Bhuiyan, M. Mahbubur Rahman

PII: S0040-6090(16)30114-6
DOI: doi: [10.1016/j.tsf.2016.04.033](https://doi.org/10.1016/j.tsf.2016.04.033)
Reference: TSF 35166

To appear in: *Thin Solid Films*

Received date: 22 October 2015
Revised date: 18 April 2016
Accepted date: 19 April 2016



Please cite this article as: Humayun Kabir, A.H. Bhuiyan, M. Mahbubur Rahman, Understanding the Charge Carrier Conduction Mechanisms of Plasma-Polymerized 2-Furaldehyde Thin Films via DC Electrical Studies, *Thin Solid Films* (2016), doi: [10.1016/j.tsf.2016.04.033](https://doi.org/10.1016/j.tsf.2016.04.033)

This is a PDF file of an unedited manuscript that has been accepted for publication. As a service to our customers we are providing this early version of the manuscript. The manuscript will undergo copyediting, typesetting, and review of the resulting proof before it is published in its final form. Please note that during the production process errors may be discovered which could affect the content, and all legal disclaimers that apply to the journal pertain.

Understanding the Charge Carrier Conduction Mechanisms of Plasma-Polymerized 2-Furaldehyde Thin Films via DC Electrical Studies

Humayun Kabir^{a,b,*}, A.H. Bhuiyan^c, M. Mahbubur Rahman^d

^aDepartment of Physics, Jahangirnagar University, Savar, Dhaka 1342, Bangladesh

^bSchool of Metallurgy and Materials, University of Birmingham, Edgbaston, Birmingham B15 2TT, United Kingdom

^cDepartment of Physics, Bangladesh University of Engineering & Technology, Dhaka 1000, Bangladesh

^dSurface Analysis and Materials Engineering Research Group
School of Engineering & Information Technology, Murdoch University, Perth,
Western Australia 6150, Australia

Corresponding Author's email: HXK598@bham.ac.uk

Abstract

Monomer 2-furaldehyde (FDH) was deposited onto the glass substrates in optimum conditions via a glow discharge using a capacitively coupled parallel plate reactor to obtain plasma polymerized 2-furaldehyde (PPFDH) thin films of different thicknesses. In order to realize the carrier conduction mechanisms, the direct current density against applied voltage (J - V) characteristics of these films with different thicknesses were investigated at different temperatures (T) in the voltage region from 0.5 to 49 V in Al/ PPFDH/Al sandwich configuration. The J - V characteristics at various temperatures follow a power law of the form $J \propto V^n$. In the low voltage region the values of n were recorded to be $0.80 \leq n \leq 1.12$ and those in the high voltage region found to lie between $1.91 \leq n \leq 2.58$, demonstrating the Ohmic conduction mechanism in the low voltage region and non-Ohmic conduction in the high voltage region. Theoretically calculated and experimental results of Schottky (β_s) and Poole-Frenkel (β_{PF}) coefficients display that the most probable conduction mechanism in PPFDH thin films is the Schottky type. Arrhenius plots of J vs. $1/T$ for an applied voltage of 5 V, the activation energies were 0.13 ± 0.02 and 0.50 ± 0.05 eV in the low and high temperature regions, respectively. However, for an applied voltage of 35 V,

the activation energy values were found to be 0.11 ± 0.01 eV and 0.55 ± 0.02 eV, respectively in low and high temperature regions.

Keywords: 2-furaldehyde, Plasma polymerization, Direct current electrical property, Ohmic conduction, Schottky emission, Activation energy.

1. Introduction

Plasma polymerization is one of the neoteric techniques that can be used to synthesize thin polymer films from a variety of organic compounds. These thin films differ slightly from conventional polymers in terms of their structure and morphology, but retain the majority of properties. Plasma polymerized thin films are preferable due to excellent coating adhesion onto a wide variety of substrates, chemical, mechanical and thermal stability and high cross linked, insoluble and pinhole-free characteristics [1-3]. It is possible to adapt the film properties to different applications by changing the deposition parameters such as reactor pressure, plasma power, flow rate, and reactor geometry [4-6]. Homogeneous, chemically inert, highly adhering, pinhole-free plasma polymerized thin films have applications in diodes, thin film transistors, switching elements, photovoltaics, microelectronics, optoelectronics, different sensors, biomedical appliances, thin film lenses, membrane separation, aerospace automobile fields, rechargeable batteries, dielectrics, light guide materials, coatings and insulating layers, etc. [7-14]. Therefore, it is extremely useful to develop high quality polymer thin films for a variety of important applications. As a consequence, the structural, electronic, optical, electrical, etc. properties of organic polymer thin films as advanced materials have received particular attention from solid state and materials scientists.

Over the years various synthesis techniques have been used to produce optical thin films with improved properties for many different technological applications e.g., photovoltaics, thermal collectors, photovoltaic thermal solar panels, and solar selective absorbers etc. Owing to its simplicity the plasma polymerization technique has been adopted for the synthesis of the coatings. This method is quick, cost effective, better compositional uniformity at low temperatures and conformational coverage in the case of films produced via solid state synthesis routes. In view of

these facts, development of convenient and environmental friendly route, higher stability and high performance thin films is always very crucial.

In direct current (DC) electrical conduction mechanisms, such as, Schottky [15], Poole-Frenkel (PF) [16] and space charge limited conduction (SCLC) [17] processes for electronic type conduction to be operative in different organic polymer thin films. Matin et al. [15] investigated the electrical transport mechanism of plasma polymerized 2, 6, diethylaniline (PPDEA) thin films and reported that at a low operating voltage, current conduction obeys the Ohm's law. The thickness dependence of current density (J) in the higher voltage region is governed by a Schottky type conduction mechanism. They also investigated the temperature dependence of the J for different bias voltages and confirmed the possibility of Schottky emission in PPDEA thin films. Sarker et al. [18] reported that in the higher voltage region, the dominant mechanism of conduction in plasma polymerized 1-Benzyl-2-methylimidazole (PPBMI) thin films is of SCLC type. The activation, carrier mobility, free charge carrier density and trap density associated with the conduction mechanism were found to be 0.43 eV, 1.48×10^{-18} to $6.35 \times 10^{-18} \text{ m}^2 \text{ V}^{-1} \text{ s}^{-1}$, 1.59×10^{23} to $5.85 \times 10^{23} \text{ m}^{-3}$ and 2.50×10^{24} to $5.00 \times 10^{23} \text{ m}^{-3}$, respectively. In another study, the effect of iodine doping on DC electrical conduction mechanism in plasma polymerized PPDEA thin films found the PF conduction mechanism is functioning [19]. Electrical conduction mechanism by J - V measurements of plasma polymerized N, N, 3, 5 tetramethylaniline, deposited via a capacitively coupled plasma polymerization method showed that the electrical transport mechanisms associated was of SCLC type [20]. Kamal et al. [21] studied the DC electrical conduction mechanism in plasma polymerized pyrrole (PPPy) thin films is mostly dominant by the SCLC kind. Sharma et al. [22] reported electrical and photovoltaic behavior of furfural resin thin films. The J - V characteristics demonstrate the ohmic conduction in the low voltage region while space charge limited conduction is dominant in the high voltage region. In another article [23], the mechanism of electrical conduction in plasma polymerized furan films predicted that there is a clear dominance of Schottky conduction. The Schottky conduction mechanism was also found to be dominant in plasma polymerized furfural thin films [24]. The structural and optical properties of these thin films have been cited elsewhere [25].

In the present study 2-furaldehyde (FDH) is chosen as the monomer because as, FDH is a derivate of furan, it is expected to yield polymer films with interesting properties in a plasma discharge. Till date, elaborate reports on the synthesis mechanisms and electrical properties of DC plasma polymerized FDH (PPFDH) thin films are scant. Viewing these facts, this paper focuses on the preparation of PPFDH thin films and investigates their DC electrical characteristics to realize the most dominant charge carrier conduction mechanisms operative under the applied DC fields. The theoretical and experimental values of Schottky (β_s) and Poole-Frenkel (β_{PF}) coefficients were estimated.

2. Experimental Details

2.1 The monomer and formation of polymer

The monomer, 2-furaldehyde (FDH) made by BDH Laboratory, BH15, (England) was procured from the local market. The chemical structure of the monomer ($C_5H_4O_2$) is shown in Fig.1. The molecular mass, density and boiling point of the monomer were estimated to 0.096 kg/mol, 1160 kg/m³ and 434.7 K, respectively. In the plasma polymerization process, the monomer, 2-furaldehyde gases were pumped into the vacuum chamber where it is polymerized by plasma to form a thin and clear coating. The starting liquid monomers were converted into gases phase in an evaporator and pumped into the vacuum chamber where the polymerization process was initiated by glow discharge. The excited electrons generated onto the glow discharge helped to ionize the monomer molecules. The monomer molecules were fragmented to create free electrons, ions, exited molecules and radicals and were absorbed, condensed and polymerized onto the glass substrates. Finally, with the deposited molecules, the electrons and ions were cross-linked to form chemical bonds and dense-hard polymer films. The empirical molecular formula of the polymer is $C_{3.60}H_{11.97}O_{1.40}$.

2.2 Preparation of thin films and thickness measurement

The FDH vapor was injected into the glow discharge reactor through a flow meter (Glass Precision Engineering, Meterate, England) at a flow rate of about 20

ml/min. The glow discharge system is a bell-jar type capacitively coupled system consisting of two stainless steel parallel plate electrodes of diameter and thickness 0.09 and 0.001 m, respectively, placed 0.04 m apart. A schematic diagram of the plasma polymerization set up is portrayed in Fig. 2 [4]. The glow discharge chamber was evacuated by a rotary pump (Vacuu brand, Germany). Glow discharge plasma was generated around the substrates, which were kept on the lower electrode, using a step up transformer connected to the electrode with different operating power, such as 30 W, 40 W and 50 W at a line frequency of 50 Hz. A base pressure maintained was 1.33 Pa while the pressure of the deposition chamber was maintained at 13.3 Pa at room temperature. Transparent and colored PPFDH thin films were deposited on the glass substrates at different deposition time (30-90 min) to obtain a suitable film thicknesses ranging from 150 to 330 nm. A plot of thickness versus deposition time at various plasma powers is printed in Fig. 3 to understand the growth kinetics of PPFDH films. It is observed that at 30 W, the plasma is low to attain film thickness satisfactorily while at 50 W; the plasma is very high, resulting a slower deposition of the films with increasing time. However, it is viewed that proper polymerization occurs at 40 W, which recommends to prepare PPFDH thin films at suitable thickness for several measurements [26].

The thickness of the films, d was measured by the multiple-beam interferometry technique [27] via following relation,

$$d = \frac{\lambda b}{2a} \quad (1)$$

where λ (= 589.3 nm) is the wavelength of monochromatic sodium light source, b the step height and a the width of the Fizeau fringes. A traveling microscope was used to measure the value of b and a formed due to the interference of light reflected from the glass and surfaces of thin films. The Fizeau fringe patterns of PPFDH films are displayed in Fig. 4. In addition to the glass substrates, another separate glass slide was used to measure the thickness of the films. Teflon tape was used to cover 50% area of the cleaned glass, which was not exposed to plasma environment during plasma polymerization. After deposition, the teflon tape was carefully removed from the glass slides. The optimized deposition conditions for the synthesis of the films are shown in Table 1.

2.3 Scanning electron microscopy

For SEM and EDX analyses, PPFDH thin films were deposited onto small pieces of chemically cleaned glass substrates. Two samples of each thickness were selected out for the analysis. To avoid the charging effect, the PPFDH thin films were coated with a thin layer of gold by sputtering (AGAR Auto Sputter Coater). The SEM and EDX analyses were performed by a scanning electron microscope (Model: S-3400N, Hitachi, Japan). The SEM machine was operated at 20 kV. In EDX, a spectrum starting from very low to high voltage (say, from 0.1 to 40 kV) can be recorded in a relatively short time (10~100 s) for a quick analysis of the elemental compositions of the specimen. SEM machine connected with an EDX analysis column with a maximum EHT (extra high tension) voltage field emission gun of 30 kV.

2.4 DC electrical measurements

For electrical measurements, aluminum (Al) contact electrodes were deposited via Edward coating unit (Model: E-306A, Edward, UK) at a chamber pressure of about 1.33×10^{-3} Pa, on both sides of the PPFDH thin films. The *J-V* characteristics of thin films of different thicknesses were studied in an Al/PPFDH/Al sandwich configuration in the DC voltage range of 0.5-50.0 V with an effective Al electrode area of 10^{-4} m² at temperatures 298, 348, 398 and 423 K. The dimensions of the PPFDH films were approximately $(1.5 \times 1.5) 10^{-4}$ m². The current across the thin films was measured using a high impedance electrometer (Model: 614, Keithley Instruments Inc., USA) and the DC voltage was supplied step by step through a stabilized DC power supply (Model: 6545A, Agilent, Malaysia). The temperature of the samples was recorded by a Chromel-Alumel thermocouple kept very close to the sample connected to a digital micro-voltmeter (Model: 197A, Keithley Instruments Inc., USA). The measurements were carried out under dynamic vacuum of about 1.33 Pa to avoid any ambient effects.

3. Results and Discussion

3.1 Surface morphology and elemental analysis

The SEM and EDAX spectra of PPFDH films were recorded at different magnifications (50k \times , 100k \times) at an accelerating voltage of 25 kV are shown in Fig. 5

and Fig. 6, respectively. The SEM images show that the surfaces of the plasma polymerized films are uniform. Our studies were found to be consistent with earlier report [28]. The EDX results indicate that carbon (C) has the highest percentage (60.60 %) and the presence of oxygen (O) follows a very good ratio as the monomer. The higher percentage (22.50 %) of oxygen in the polymer is due to the due to the combination of contributions from the glass substrates and atmospheric oxygen when samples were taken out side of the reactor chamber. The presence of sodium and silicon as detected in EDAX studies of the films were not found in the monomer FDH might be appearing from the glass substrates. However, EDAX was unable to identify the presence of hydrogen in PPFDH films [15].

3.2 Electrical Properties of PPFDH Films

3.2.1 *J-V characteristics*

The *J-V* characteristics of PPFDH films with 160, 220, 280 and 330 nm thicknesses at temperatures of 298, 348, 398 and 423 K in the voltage range of 0.5 to 50 V are represented in Fig. 7. Fig. 7 shows that the *J-V* characteristics follow a power law of the form $J \propto V^n$ with different values of 'n' (slopes), where *n* is a power factor. In the low voltage region the value of slopes lies between $0.79 \leq n \leq 1.12$ while that in the high voltage region falls in the range of $1.81 \leq n \leq 2.58$ as shown in Table 2. These features point out that the current conduction is of Ohmic nature in the low voltage region and non-Ohmic in the high voltage region [15]. Furthermore, at the higher temperatures regions the values of *J* increases significantly, revealing a strong temperature dependence of *J*.

3.2.2 *Conduction mechanism in PPFDH thin films*

Charge injected from a metal to an insulator or a semiconductor at medium electric fields, generally, occurs by field-assisted thermionic emission, a process known as the Richardson-Schottky effect or simply, a Schottky emission. This is a process of image force induced lowering of the potential energy for charge carrier emission under an applied electric field [29]. As a result of the image force, the potential step changes smoothly at the metal-insulator interface. The other process is

called PF generation where carriers are produced by the dissociation of donor–acceptor centers in the bulk of the material due to field-enhanced thermal excitation of trapped electrons into the conduction band. [30]. If the generation process is slower than the transport by the carriers through the material, the conduction is governed by generation, specifically by either the Schottky, or PF mechanism. Conversely, when the transport is slower than generation, it constitutes the rate-determining step, and the conduction is described by the theory of SCLC. If a charge is injected at the electrode–polymer interface, a large excess carrier density at the injecting electrode exists and an SCL current flows [31].

The steady-state SCL current density obeys an equation of the form [32],

$$J = \frac{9\mu\varepsilon'\varepsilon_0 V^2}{8d^3} \quad (2)$$

where ε' is the dielectric constant of the material, ε_0 the permittivity of the free space, μ the mobility of charge carriers and d the thickness of the thin film. Therefore, for SCLC mechanisms, the slope of the J - V characteristics should be greater than or equal to 2. As seen from the J - V plots in Fig. 7, in the higher voltage region the estimated values of n are $1.81 \leq n \leq 2.58$, which suggest the possibility of presence of SCLC or PF or Schottky type mechanism in the PPFDH films. According to SCLC theory [33], the thickness dependence of the SCLC follows the relation $J \propto d^m$, where m is a parameter which depends on the trap distribution and is equal to or greater than 3 in the presence of traps. The thickness dependence of the J for PPFDH films is exposed in Fig. 8. It can be seen from Fig. 8 that J varies as $d^{2.7}$. The value 2.7 is much less than the required exponent value for SCLC. So, SCLC conduction mechanism is ruled out.

The general expression for both Schottky and PF type conduction is expressed as [34],

$$J = J_0 \exp\left(\frac{\beta F^{1/2} - \phi}{kT}\right) \quad (3)$$

In this equation J_0 is the low-field current density; F , the applied electric field; k , the Boltzmann constant; T , the absolute temperature and ϕ , the ionization energy of localized centers in PF conduction and Coulomb barrier height of the electrode polymer interface in Schottky type conduction and β , the coefficient of the static

electric field. The coefficient β for the Schottky type conduction is known as the Schottky coefficient (β_s) and is defined as,

$$\beta_s = \left(\frac{e^3}{4\pi\epsilon'\epsilon_0} \right)^{1/2} \quad (4)$$

For the PF mechanism, it is called the PF coefficient (β_{PF}) and is defined as,

$$\beta_{PF} = 2 \left(\frac{e^3}{4\pi\epsilon'\epsilon_0} \right)^{1/2} = 2\beta_s \quad (5)$$

where, e is the electronic charge. Therefore according to Eq. (2) a plot of $\text{Log}(J)$ versus $V^{1/2}$ (Schottky plots) should be a straight line in the higher voltage region with a positive slope. Fig. 9 presents the plots between $\text{Log}(J)$ versus $V^{1/2}$ for PPFDH films with different thicknesses. These Schottky plots are almost straight lines with positive slopes demonstrating the probable conduction mechanism to be of Schottky or PF type. Thus, from the voltage dependence of current density data at different temperatures, it is confirmed that the mechanism of charge transport in PPFDH films is either due to Schottky or PF type. To differentiate between these two conduction mechanisms, β_s and β_{PF} were calculated theoretically and compared them with the experimental results. The relation $\beta_{\text{expt}} = p k T d^{1/2}$ was used for experimental evaluation of β , where, p is the slope ($p = \Delta \text{Ln } J / \Delta V^{1/2}$) of the $\log(J)$ vs $V^{1/2}$ graph. However, the theoretical values of β were calculated using Eqs. (4) and (5) and the values are set out in Table 3. From Table 3, it can be seen that the values of β_{exp} are close to the values of β_{th} which indicate that the probable mechanism of charge transport in the PPFDH film is of the Schottky type. Furthermore, in the Schottky-Richardson mechanisms, the J shows strong temperature (T) dependence but not in the case of PF mechanisms. Another alternative way to recognize whether the conduction mechanism is of PF or Schottky type, is to inspect the temperature dependence of the current density.

3.2.3 Temperature dependence of current density

The temperature dependence of the J is expressed by the Arrhenius law,

$$J = J_0 \exp\left(-\frac{\Delta E}{kT}\right) \quad (6)$$

where J_0 is a constant, ΔE , the thermal activation energy of electrical conduction and k , the Boltzmann constant. Fig. 10 illustrates the dependence of J on inverse absolute temperature, $1/T$, for PPFDH films of thicknesses 160, 220, 280 and 330 nm. The temperature dependence studies of J were carried out both in the low voltage ($V=5V$) and high voltage ($V=35V$) regions. At temperature $T < 340$ K, the J increases slowly and above this temperature J increases rapidly. This increase in J with T is associated with the increased movement of the ions and/or electrons. Further observations show that both curves are characterized by two different slopes in the low and high temperature regions. The curves have varying slopes at low temperatures but become almost linear in the high temperature region, corresponding to well-defined ΔE . The activation energies associated with two temperature regions were calculated from the slopes of the J - $1/T$ plots and are illustrated in Table 4. At an applied voltage of 5V in the low temperature regions, the activation energies are found to be 0.13 ± 0.02 eV and at higher temperature regions it is 0.50 ± 0.05 eV, whereas, in the low and high temperature regions activation energies were found to be 0.11 ± 0.01 eV and 0.55 ± 0.02 eV, respectively for an applied voltage of 35 V. These small values of the activation energies in the low and high temperature regions suggest the existence of the shallow trap levels in PPFDH films. The low activation energies in the low temperature regions signpost that the thermally activated hopping conduction is operative in this material. This change in ΔE from lower to higher values may be attributed to a transition from a hopping regime to a regime dominated by distinct energy levels [35].

4. Conclusions

Glow discharged plasma polymerized PPFDH films deposited onto the glass substrates were studied to realize their DC electrical conductivity mechanisms. SEM studies show that the surfaces of the PPFDH film are uniform and pinhole free. The

EDAX results imply the existence of C, O, Na and Si. However, Na and Si were originated from the glass substrates. A comparison, between the theoretically calculated values of the coefficient of the static electric field, β associated with the Schottky, β_s and PF, β_{PF} were type of conduction mechanisms with that of the experimentally measured values led that the conduction mechanism in PPFDH films is concomitant by the Schottky type. The Schottky type mechanism was also established by the temperature dependence studies of the current density.

Acknowledgements

The financial support of Bangladesh University of Engineering & Technology (BUET) is thankfully acknowledged by H. Kabir. H. Kabir also gratefully acknowledges Jahangirnagar University for providing with the permission to carry out this work. M.M. Rahman is supported by Murdoch University.

References

- [1] N. Inagaki, S. Kondo, M. Hirata, H. Urushibata, Plasma polymerization of organosilicon compounds, J. Appl. Polym. Sci. 30 (1985) 3385-3395.
- [2] Y. Inoue, H. Sugimura, O. Takai, In situ observation of behavior of organosilicon molecules in low-temperature plasma enhanced CVD, Thin Solid Films 345 (1999) 90-93.
- [3] F.-U.-Z. Chowdhury, A.H. Bhuiyan, Dielectric properties of plasma-polymerizeddiphenyl thin films, Thin Solid Films 360 (2000) 69-74.
- [4] T. Afroze, A.H. Bhuiyan, Effect of heat treatment on the structural and optical characteristics of plasma deposited 2-(diethylamino) ethyl methacrylate thin films by a capacitively coupled glow discharge plasma system, Phys. Scr. 88 (2013) 045502.
- [5] C. Bourreau, Y. Catherine, P. Garcia, Plasma enhanced chemical vapor depositionof hexamethyldisiloxane deposited by a room temperature PECVD process in a parallel plate reactor, Plasma Chem. Plasma Process. 10 (1990) 247-260.

- [6] K.W. Gerstenberg, Film deposition in a radial flow reactor by plasma polymerization of hexamethyldisilazane, *Colloid. Polym. Sci.* 268 (1990) 345-355.
- [7] H. Xiao, X. Zhao, A. Uddin and C.B. Lee, Preparation, characterization and electronic and optical properties of plasma-polymerized nitriles, *Thin Solid Films* 477 (2005) 81-87.
- [8] S. Mutlu, D. Çokeliler, A. Shard, H. Goktas, B. Ozansoy, M. Mutlu, Preparation and characterization of ethylenediamine and cysteamine plasma polymerized films on piezoelectric quartz crystal surfaces for a biosensor, *Thin solid films* 516 (2008) 1249-1255.
- [9] H. Yatsuda, M. Nara, T. Kogai, H. Aizawa and S. Kurosawa, STW gas sensors using plasma-polymerized allylamine, *Thin Solid Films* 515 (2007) 4105-4110.
- [10] X.Y. Zhao, M.Z. Wang, J. Xiao, Deposition of plasma conjugated polynitrile thin films and their optical properties, *Eur. Polym. J.* 42 (2006) 2161-2167.
- [11] R.d'Agostino(Ed.), *Plasma Deposition, Treatment and etching of polymers*, Academic Press, Boston, 1990.
- [12] N. Guermat, A. Bellel, S. Sahli, Y. Segui, P. Raynaud, Thin plasma-polymerized layers of hexamethyldisiloxane for humidity sensor development, *Thin Solid Films* 517 (2009) 4455-4460.
- [13] M. Nakamura, L. Sugimoto, H. Kuwano, Application of plasma-polymer-film-coated sensors to gas identification using linear filters, *Sens. Actuators B: Chem.* 33 (1998) 122-127.
- [14] H. Muguruma, Plasma-polymerized films for biosensors II, *Tr. Anal. Chem.* 26 (2007) 433-443.
- [15] R. Matin, A.H. Bhuiyan, Electrical transport mechanism in plasma polymerized 2, 6, diethylaniline thin films, *Thin Solid Films* 519 (2011) 3462-3467.
- [16] A.B.M. Shah Jalal, S. Ahmed, A.H. Bhuiyan, M. Ibrahim, On the conduction mechanism in plasma polymerized m-xylene thin films, *Thin Solid Films* 295 (1997), 125-130.
- [17] M. Zaman, A.H. Bhuiyan, Direct current electrical conduction mechanism in plasma polymerized thin films of tetraethylorthosilicate, *Thin Solid Films* 517 (2009) 5431-5434.

- [18] R.B. Sarker, A.H. Bhuiyan, Electrical conduction mechanism in plasma polymerized 1-Benzyl-2-methylimidazole thin films under static electric field, *Thin Solid Films* 519 (2011) 5912-5916.
- [19] R. Matin, A.H. Bhuiyan, Effect of iodine doping on the electrical transport mechanism in plasma polymerized 2,6-diethylaniline thin films, *J. Phys. And Chem. Solids* 75 (2014) 198-202.
- [20] H. Akther, A.H. Bhuiyan, Electrical and optical properties of plasma-polymerized N, N, 3, 5-tetramethylaniline thin films, *New J. Phys.* 7 (2005) 173.
- [21] M.M. Kamal, A.H. Bhuiyan, Direct current electrical conduction mechanism in plasma polymerized pyrrole thin films, *J. Mod. Sci. Technol.* 2 (2) (2014) 1-9.
- [22] G.D. Sharma, S.G. Sandogaker, M.S. Roy, Investigation of electrical and photovoltaic behaviour of furfural resin thin film devices, *Phys. Status Solidi A* 158 (1996) 599-610.
- [23] D.S. Kumar, On the mechanism of electrical conduction in plasma polymerized furan films *J. Mat. Sci.* 35 (2000) 4427- 4430.
- [24] C. Joseph Mathai, M.R. Anantharaman, S. Venkitachalam, S. Jayalekshmi, Mechanism of electrical conduction in plasma polymerized furfural thin films, *Thin Solid Films* 416 (2002) 10-15.
- [25] H. Kabir, M.M. Rahman, T.S. Roy, A.H. Bhuiyan, Structural and optical properties of plasma polymerized pyromucicaldehyde thin films, *Int. J. Mechan. Mechatron. Eng.* 12 (5) (2012) 30-34.
- [26] R. Matin, A.H. Bhuiyan, Infrared and ultraviolet-visible spectroscopic analyses of plasma polymerized 2,6 diethylaniline thin films, *Thin Solid Films* 534 (2013) 100-106.
- [27] S. Tolansky, Multiple beam interferometry of surfaces and films, Clarendon Press, Oxford, 1948.
- [28] M.J. Rahman, A.H. Bhuiyan, Structural and optical properties of plasma polymerized o methoxyaniline thin films, *Thin Solid Films* 534 (2013) 132-136.
- [29] S.M. Sze, Physics of Semiconductor Devices, Second Edition Wiley & Sons, New York, 1981.

- [30] J. Frenkel, Onpre-breakdown phenomena in insulators and electronic semi-conductors, *Phys. Rev.* 54 (1938) 647-652.
- [31] H. Yasuda, *Plasma polymerization*, Academic Press, New York, 1985.
- [32] Y. Wang, and P.B. Balbuena, Theoretical insights into the reductive decompositions of propylene carbonate and vinylencarbonate: Density functional theory studies, *J. Phys. Chem. B*, 106 (2002) 4486-4495.
- [33] D.R. Lamb, *Electrical conduction mechanisms in thin insulating films*, Methuen and Co. Ltd, London, 1967.
- [34] B. Thomas, M.G.K. Pillai, S. Jayalekshmi, On the mechanism of electrical conduction in plasma-polymerised thiophene thin films, *J. Phys. D: Appl. Phys.* 21 (1988) 503-510.
- [35] R.D. Gould, The interpretation of space-charge-limited currents in semiconductors and insulators, *J. Appl. Phys.* 53 (1982) 3353-3360.

List of Figures

Figure 1. The chemical structure of 2-furaldehyde.

Figure 2. Plasma polymerization setup: Pressure gauge (1), monomer inlet (2), monomer container (3), steel electrodes (4), to vacuum pump (5), ac power supply (6), glass cylinder (7), electrode stands (8), monomer (9), upper flange (10) and lower flange (11).

Figure 3. Variation of d with t for the PPFDH thin films at different plasma powers.

Figure 4. The Fizeau fringe pattern of PPFDH thin films.

Figure 5. SEM micrographs of the PPFDH thin films at 50k \times (a) and 100k \times (b).

Figure 6. EDAX spectra of PPFDH thin films.

Figure 7. Variation of J with V at different temperatures for PPFDH thin films, (a) $d=160$ nm, (b) $d=220$ nm, (c) $d=280$ nm, (d) $d=330$ nm.

Figure 8. Variation of J with d for PPFDH thin films.

Figure 9. Variation of $\ln J$ with $V^{1/2}$ for PPFDH thin film, (a) $d=160$ nm, (b) $d=220$ nm, (c) $d=280$ nm, (d) $d=330$ nm.

Figure 10. Variation of J with $1/T$ for PPFDH thin films in Ohmic and non-Ohmic regions, (a) $d=160$ nm, (b) $d=220$ nm, (c) $d=280$ nm, (d) $d=330$ nm.

Table Captions

Table 1. The optimum plasma polymerization conditions for PPFDH films.

Table 2. Values of ' n ' at different temperatures for PPFDH films.

Table 3. Comparison between the theoretical (β_{th}) and experimental (β_{exp}) coefficients of PPFDH films.

Table 4. Values of activation energy (ΔE) of PPFDH films at different thicknesses.

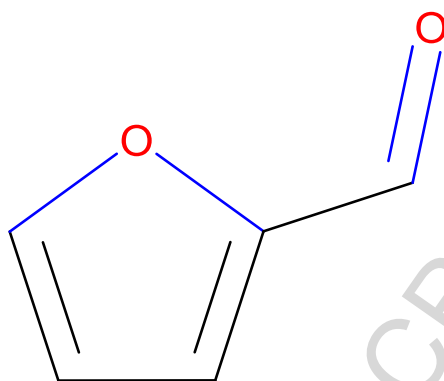


Figure 1. The chemical structure of 2-furaldehyde.

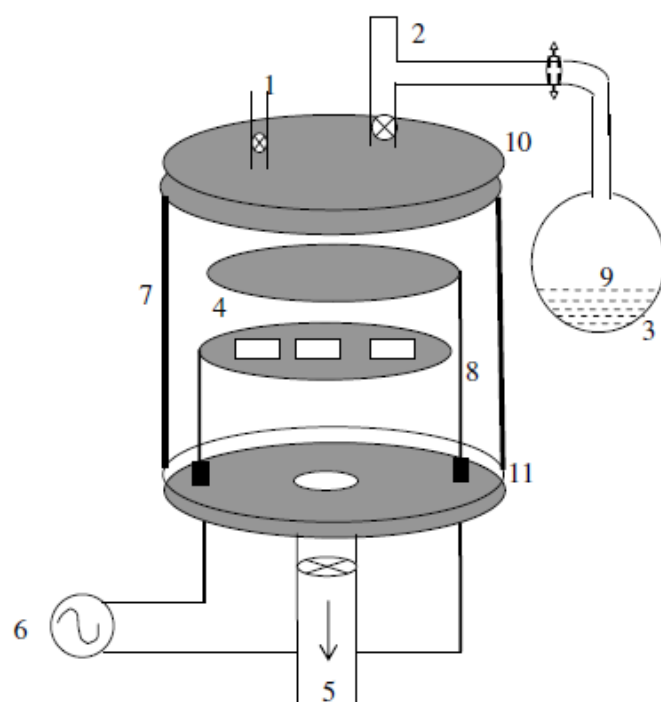


Figure 2. Plasma polymerization setup: Pressure gauge (1), monomer inlet (2), monomer container (3), steel electrodes (4), to vacuum pump (5), ac power supply (6), glass cylinder (7), electrode stands (8), monomer (9), upper flange (10) and lower flange (11).

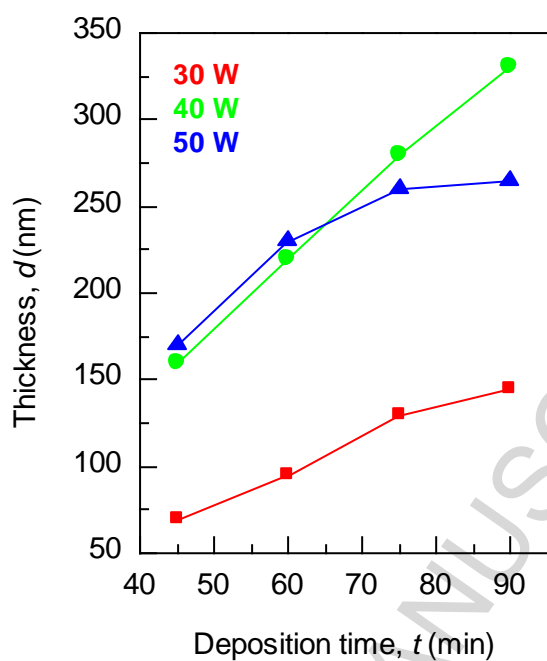


Figure 3. Variation of d with t for the PFDH thin films at different plasma powers.

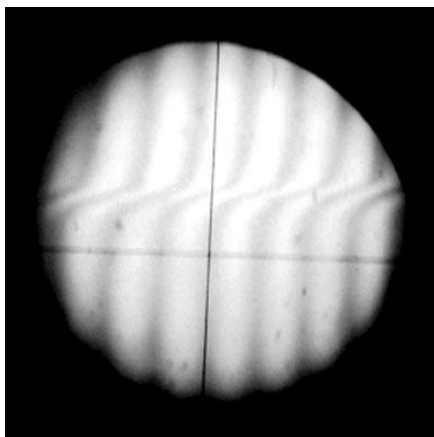


Figure 4. The Fizeau fringe pattern of PPFDH thin films.

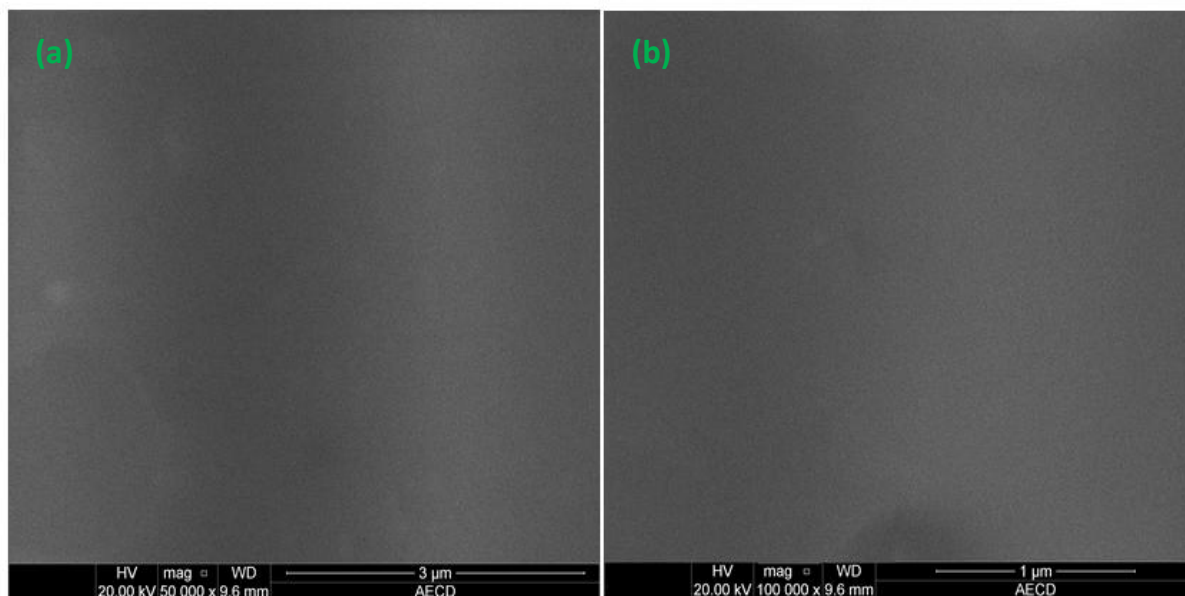


Figure 5. SEM micrographs of the PPFDH thin films at 50k \times (a) and 100k \times (b).

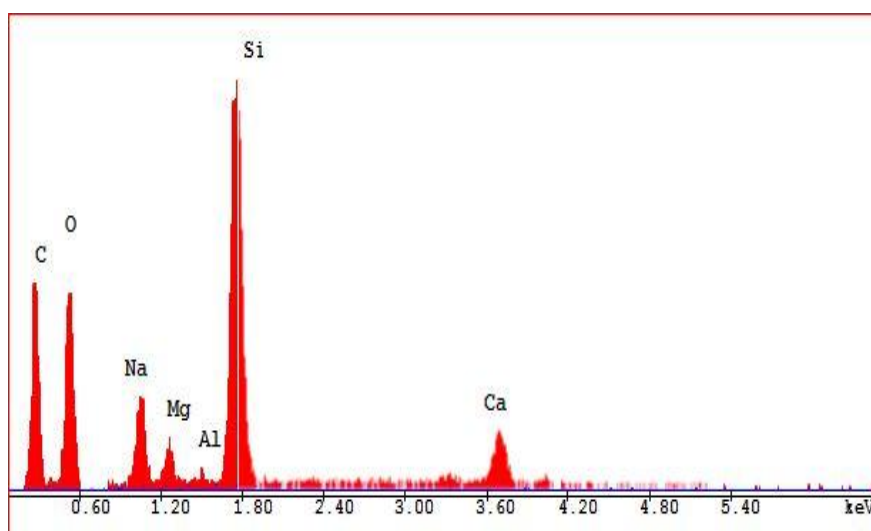


Figure 6. EDAX spectra of PPFDH thin films.

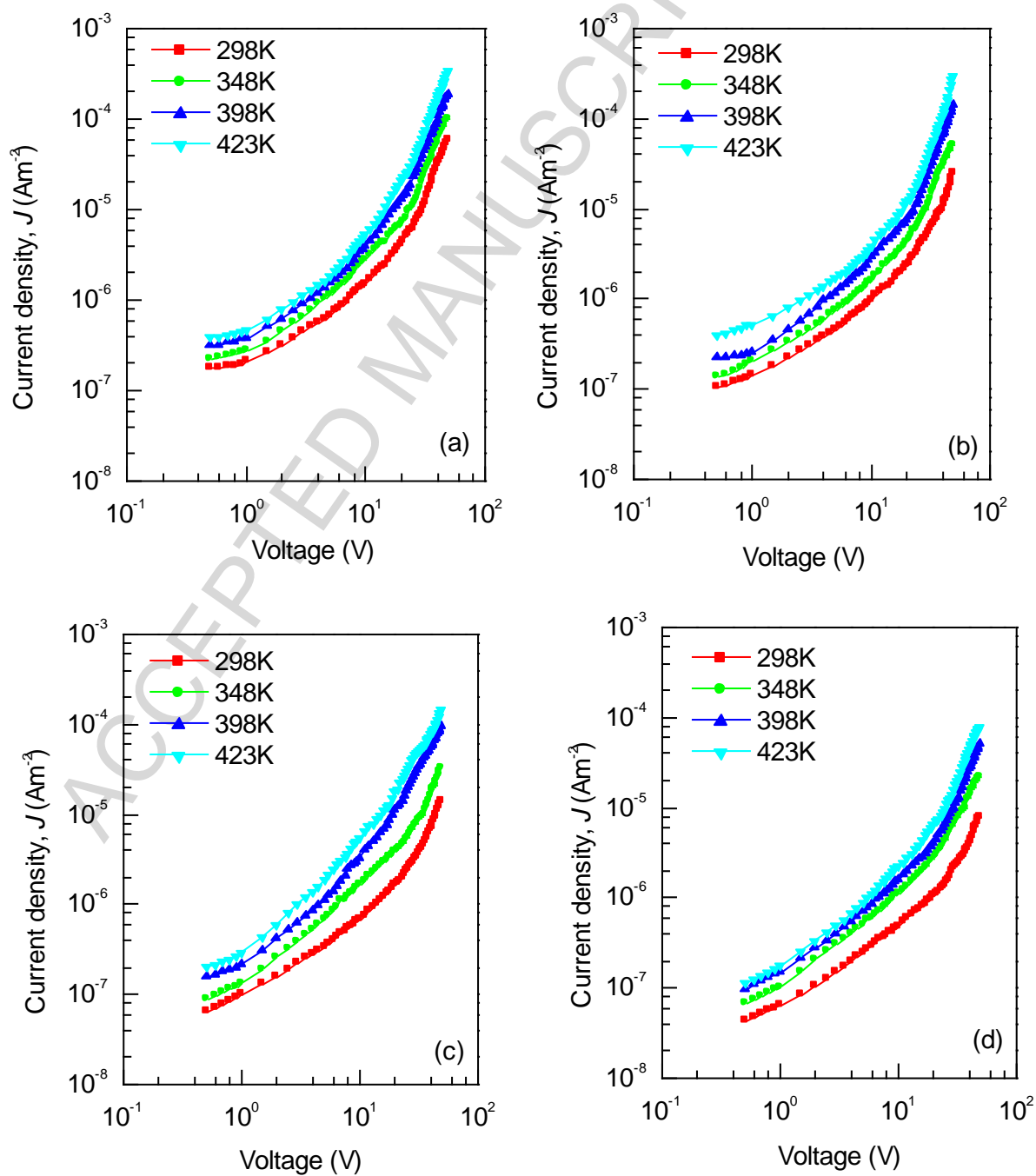


Figure 7. Variation of J with V at different temperatures for PPFDH thin films, (a) $d=160$ nm, (b) $d=220$ nm, (c) $d=280$ nm, (d) $d=330$ nm.

ACCEPTED MANUSCRIPT

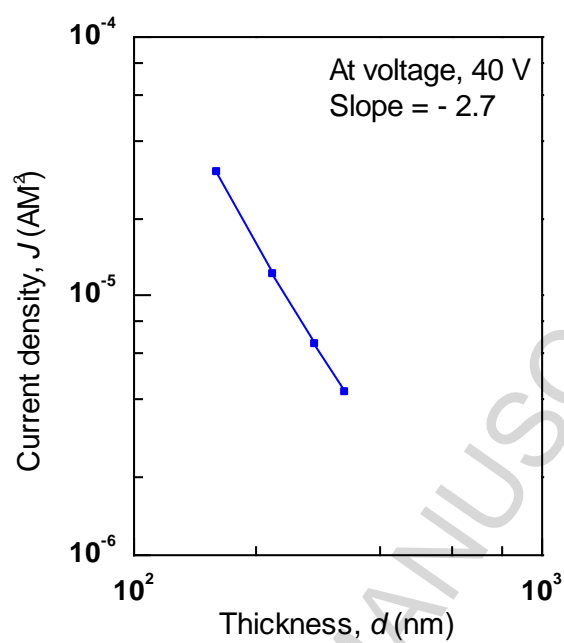


Figure 8. Variation of J with d for PPFDH thin films.

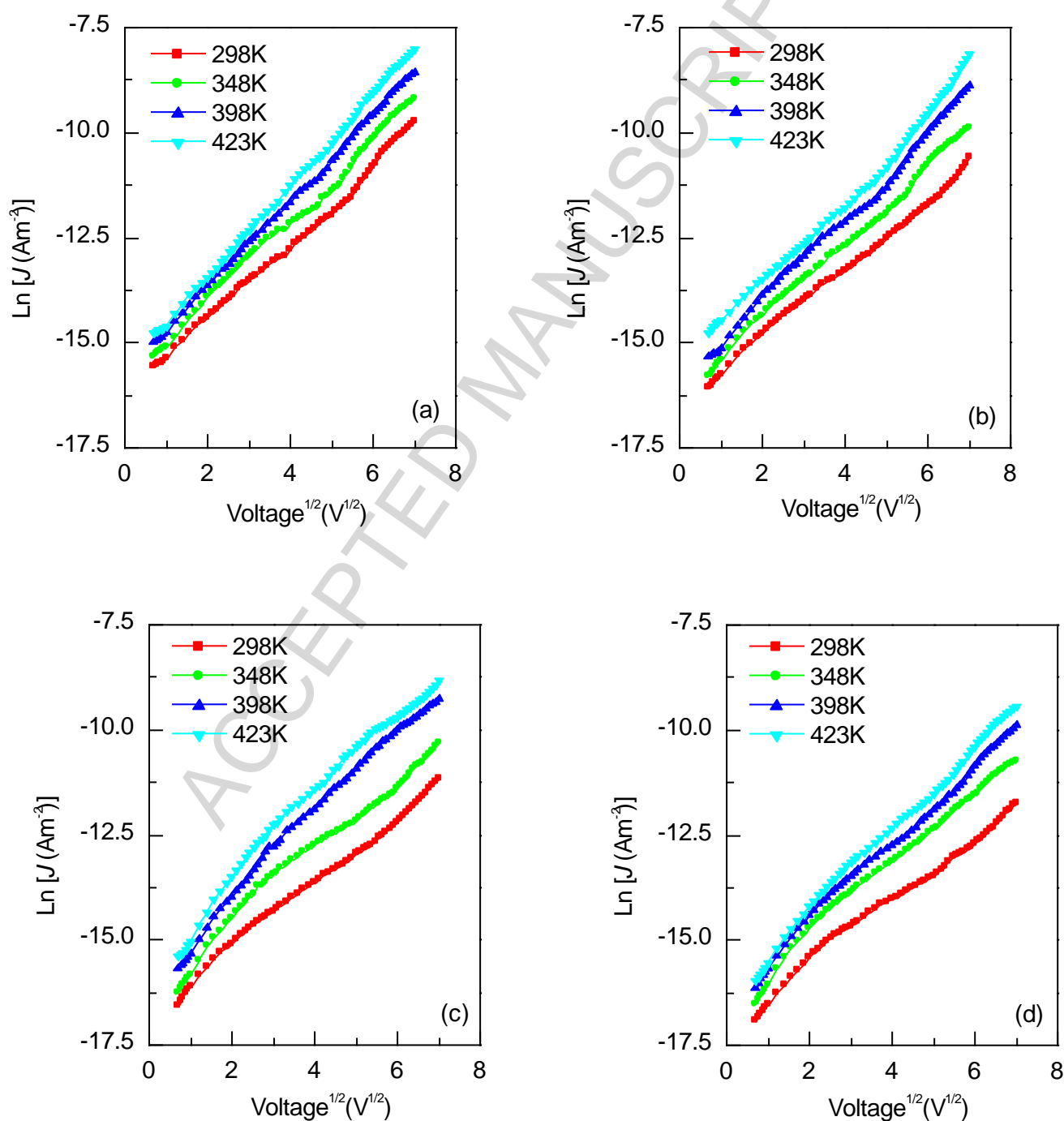


Figure 9. Variation of $\ln J$ with $V^{1/2}$ for PPFDH thin film, (a) $d=160$ nm, (b) $d=220$ nm, (c) $d=280$ nm, (d) $d=330$ nm.

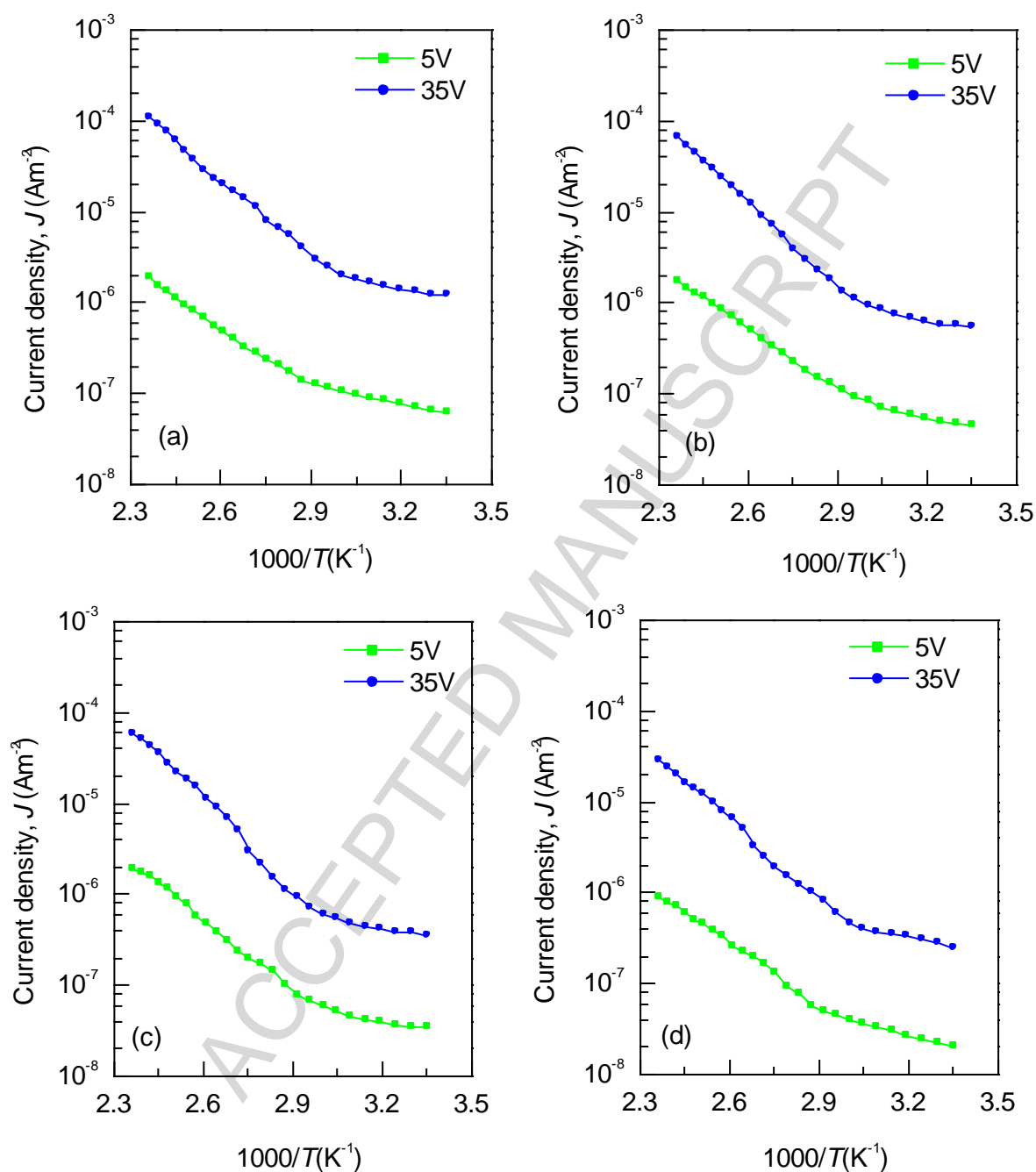


Figure 10. Variation of J with $1/T$ for PPFDH thin films in Ohmic and non-Ohmic regions, (a) $d=160$ nm, (b) $d=220$ nm, (c) $d=280$ nm, (d) $d=330$ nm.

Table 1. The optimum plasma polymerization conditions for PPFDH films.

Experimental condition	Name/Values
Separation between two electrodes	4 cm
Position of the substrate	Lower electrode
Power	40W
Base pressure in the reactor	1.33 Pa
Deposition time	40 min -90 min
Line frequency	50 Hz

Table 2. Values of ' n ' at different temperatures for PPFDH films.

Thickness, d (nm)	Temperature T (K)	Values of the slope, n	
		Low voltage region	High voltage region
160	298	0.79	1.98
	348	1.00	2.28
	398	0.94	2.29
	423	0.94	2.58
220	298	0.88	2.56
	348	1.10	2.13
	398	1.10	2.51
	423	0.99	2.58
280	298	0.80	1.96
	348	0.99	1.81
	398	1.00	2.23
	423	1.12	2.24
330	298	0.98	1.89
	348	0.99	2.02
	398	1.00	2.14
	423	1.02	2.24

Table 3. Comparison between the theoretical (β_{th}) and experimental (β_{exp}) coefficients of PPFDH films.

Thickness of the films, d (nm)	Dielectric constant (at $f = 1$ kHz)	Theoretical values		Experimental value β_{exp} ($eV \cdot m^{1/2} V^{-1/2}$)
		Schottky coefficient, β_s ($eV \cdot m^{1/2} V^{-1/2}$)	Poole-Frenkel coefficient, β_{pf} ($eV \cdot m^{1/2} V^{-1/2}$)	
160	6.7	1.47×10^{-5}	2.92×10^{-5}	1.25×10^{-5}
220	6.2	1.52×10^{-5}	3.04×10^{-5}	1.34×10^{-5}
280	5.7	1.59×10^{-5}	3.18×10^{-5}	1.40×10^{-5}
330	4.5	1.79×10^{-5}	3.58×10^{-5}	1.49×10^{-5}

Table 4. Values of activation energy (ΔE) of PPFDH films at different thicknesses.

Thickness of the films, d (nm)	Activation energy, ΔE (eV)			
	At 5 V		At 35 V	
	At low temperature	At high temperature	At low temperature	At high temperature
160	0.11	0.47	0.11	0.57
220	0.12	0.46	0.10	0.57
280	0.15	0.55	0.12	0.53
330	0.12	0.45	0.11	0.56

Highlights

- Plasma polymerized 2-furaldehyde films were synthesized via glow discharge technique.
- Uniformity of the surface of the PPDFH films were identified via SEM analysis.
- Energy dispersive X-ray spectra show the presence of C, O, and substrate related elements.
- The dominant conduction mechanism in the PPDFH films is of Schottky type.
- Schottky type mechanism was also confirmed by the temperature dependence J-V studies.